

Image conflation and change detection using area ratios

Boris Kovalerchuk*, Michael Kovalerchuk, William Sumner, Adam Haase
Dept. of Computer Science, Central Washington University, Ellensburg, WA, USA 98926-7520

ABSTRACT

The problem of imagery registration/conflation and change detection requires sophisticated and robust methods to produce better image fusion, target recognition, and tracking. Ideally these methods should be invariant to arbitrary image affine transformations. A new abstract algebraic structural invariant approach with area ratios can be used to identify corresponding features in two images and use them for registration/conflation. Area ratios of specific features do not change when an image is rescaled or skewed by an arbitrary affine transformation. Variations in area ratios can also be used to identify features that have moved and to provide measures of image registration/conflation quality. Under more general transformations, area ratios are not preserved exactly, but in practice can often still be effectively used. The theory of area ratios is described and three examples of registration/conflation and change detection are described.

Keywords: imagery registration, conflation, abstract algebra, structural algebraic invariants, area ratios, geospatial feature, change detection

1. INTRODUCTION

The development of a universal algorithm that can integrate, register, and conflate images of different and unknown rotations, translations, scaling, resolutions and modalities is an ultimate goal in the area of image integration. A recent survey¹ indicates that in spite of hundreds of algorithms developed this ultimate task of a universal algorithm remains unsolved. There are several reasons for this. One of them is in deficiencies in mathematical foundations. We offer a new promising approach based on the algebraic paradigm that differs from the more traditional geometric and topological mathematical approaches.

In previous research² algebraic methods have been based on algebraic structural analysis of features represented as open polylines called linear features. In this paper we report a new algebraic method based on ratios of areas of closed contours (shapes). It has been proven that this method is invariant to disproportional scaling and invariant to any general affine transform of the images. The method is applicable to images that contain three or more matching shapes, but those shapes and their actual matches are not known.

The algorithm has been developed using both algebraic mathematical paradigm and an **algorithm development technology for conflation (ADTC)**³. The concept of conflation has been identified by many authors¹⁻⁸. This task is an expansion of the imagery registration task⁹⁻¹². The flowchart in Figure 1 shows the general sequence of steps for the algorithm development methodology. These steps can be looped to get an improved result.

2. PARAMETER INVARIANCE

Invariance to **disproportional scaling (DPS)** is one of the most difficult requirements to meet. Such algorithm can be capable to integrate, register and conflate images that are rotated, shifted and disproportionaly scaled. It is assumed that all these factors are not known and the algorithm should discover them from the images.

To be able to build an invariant algorithm we need to discover parameters that will be invariant under disproportional

* borisk@cwu.edu; phone 1 509 963-1438; fax 1 509 963-1449; www.cwu.edu/~Imaglab/

scaling. Few invariant parameters are known. Affine Moment Invariants (AMI)¹ are among them, but AMI are not very robust to the noise in image and have some other limitations.

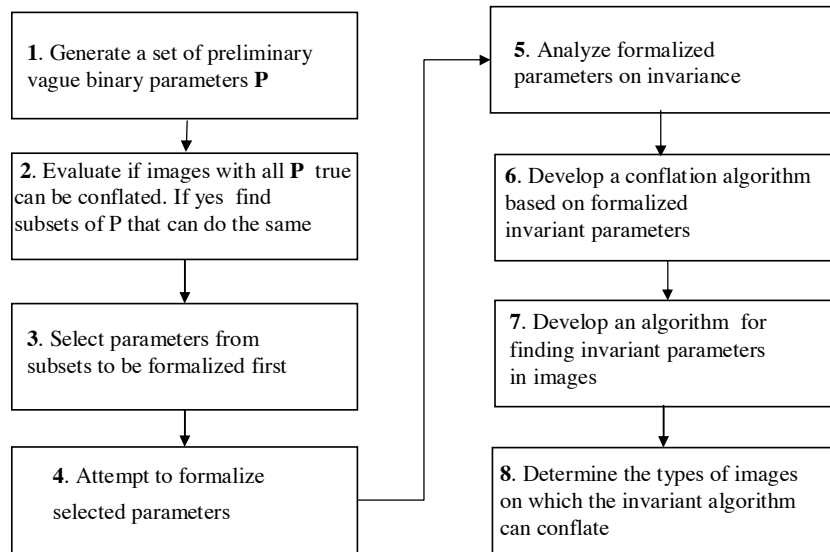


Figure 1. Overall steps of the ADTC technology

Other parameters that are typically invariant if they exist in both images are road intersections, and building corners. Extraction of both depends on image quality and if there are too many of them then there is a computational challenge to match them. If images have very different resolutions then finding matching road intersections and building corners may not be possible at all. Thus the algorithms based on these parameters may not be quite universal.

Algorithms based on AMI are potentially more universal. Such algorithms require only three matched full closed contours in each image. The algorithm that we present in this paper requires the same three matched closed contours in each image to exist.

The most fundamental difference of our method from AMI is that parameters that we use have clear and intuitive interpretation in contrast with AMI that is hard to interpret. Our parameters are **area relations and area ratios** that we discuss below. Next our parameters are more robust to noise than AMI. Another contrasting property of our algorithm is that we use as parameters the relations between two different shapes in the image. AMI algorithms use features of each single shape in the image. They are later forced because of this to use relatively arbitrary metrics for similarities between shapes. We use actual relations that exist between shapes in the image that have direct meaning in the image and direct interpretation in the image also.

Angles between linear segments of the features and lengths of those segments vary under affine transforms significantly, but their relations, $>$, $<$, $=$ are more robust. However, these relations are not complete affine invariants under disproportional scaling, but some **relations between areas are invariant**. Such invariants are also used for pattern recognition tasks¹³ that have important differences from registration and conflation tasks despite many similarities. In registration tasks we typically have many objects that can and should be matched. In recognition tasks we may need to find an object of the interest in the image.

Figures 2 and 3 show invariant features. In Figure 2, area S_1 is equal to area S_2 , $S_1=S_2$. In addition, angles A, B, and C, D are equal, $A=B$, $C=D$ too. Figure 3 presents the same image after disproportional scaling, where X coordinate was multiplied by $k_x>1$ and Y coordinate is not changed, $k_y=1$. Relations between angles A and B have been changed, $A<B$. Also relations between angles C and D are changed, $C<D$. In contrast, the relation between areas S_1 and S_2 is not changed, $S_1=S_2$. This can be proved by noticing that bounding boxes U_1 and U_2 around rhombuses S_1 and S_2 are not changed and each rhombus occupies a half of its bounding box. More formally we have $U_1=k_xk_yU_1$, $U_2=k_xk_yU_2$, and using property $U_1=U_2$, we conclude that $k_xk_yU_1=k_xk_yU_2$ and therefore $U_1=U_2$. Next, $S_1=U_1/2$ and $S_2=U_2/2$ hence $S_1=S_2$.

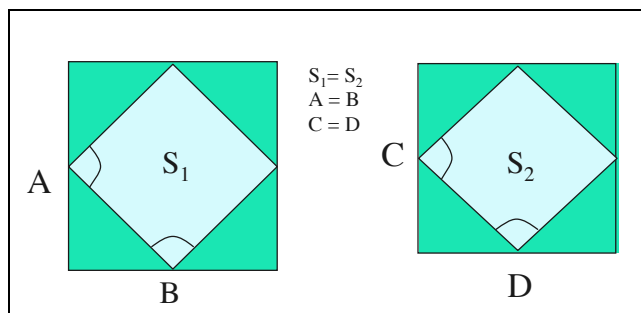


Figure 2. Original image

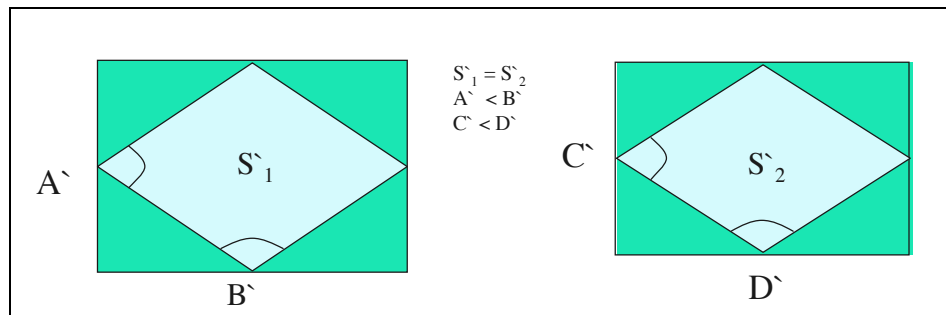


Figure 3. Image after disproportional scaling

The proof is also valid for the general case when $k_x \neq 1$. We can notice that rotation and translation do not change relations between angles as well as between areas. Thus, area relations are not changed under translation, rotation and disproportional scaling.

Above we considered only simple relations “=” and “>” between areas. Other **area functions** can also be invariants. The **ratio of areas** S_1/S_2 is also invariant under disproportional scaling, because $k_x k_y S_1/k_x k_y S_2 = S_1/S_2$. The consideration above can be converted into a formal theorem statement. Let F be an affine transformation that combines disproportional scaling transformation K with scaling coefficients (k_x, k_y) , $k_x \neq 0$, $k_y \neq 0$, translation T and rotation R , $F=KTR$, where K, T and R are transformation matrixes. Let also G_1 and G_2 be two closed regions and $S_1=S(G_1)$ and $S_2=S(G_2)$ be their areas respectively, where $S(\cdot)$ is an operator that computes area of the region G_i .

Statement: An affine transformation F of the image does not change the relation between area ratios,

$$S_1/S_2 = S(G_1)/S(G_2) = S(F(G_1))/S(F(G_2)),$$

that is, F is an **isomorphism** for area ratio $S(G_1)/S(G_2)$.

The proof follows from the considerations that preceded the theorem. If images are rotated and shifted then the theorem is true as well because rotation and shift do not change areas at all. Thus we can first rotate and shift images to made them horizontal and with the common origin. After that our previous reasoning about disproportional scaling can be applied.

For a general affine transform F

$$\begin{aligned} x' &= m_{11}x + m_{12}y + m_{13} \\ y' &= m_{21}x + m_{22}y + m_{23} \end{aligned} \tag{1}$$

and arbitrary shapes we can explain the idea of the proof of this theorem in the following way. Any shape can be interpolated by a set of rectangles such as horizontal black rectangles shown in Figure 4. Then we can apply a general affine transform F to the image that will transform each rectangle into another rectangle.

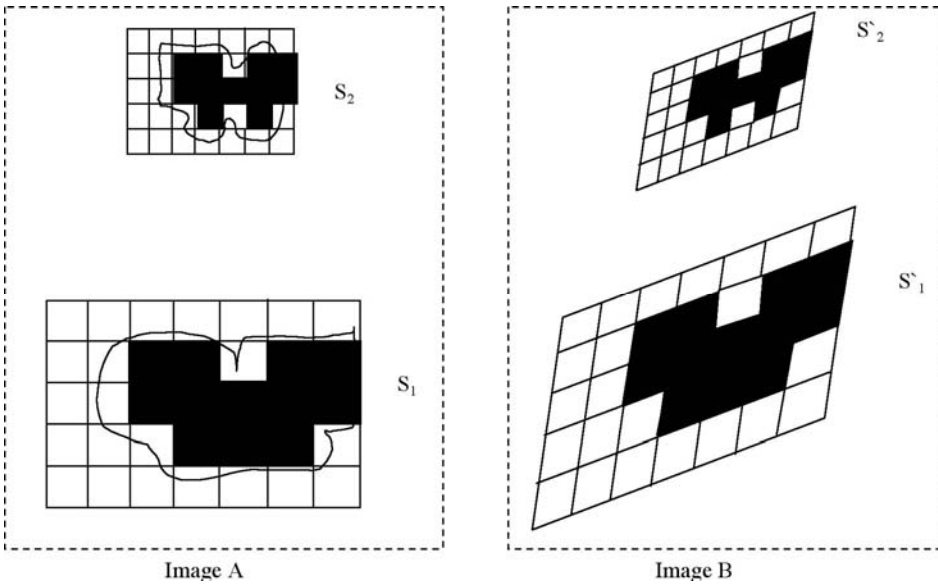


Figure 4. General affine transform

Figure 4 explains the idea of the proof for a general affine transform F . We have black shapes S_1 , S_2 and shapes S'_1 and S'_2 after applying F to the image A that contains both S_1 and S_2 . The ratio S_1/S_2 is equal to $12k/11$ by counting black squares in S_1 and S_2 , where k is a ratio of sizes of squares. In this example four small squares form a large square, thus $k=4$. In image B the ratio S'_1/S'_2 is equal to $m12/11$ again by counting black distorted squares in S'_1 and S'_2 , where m is a ratio of sizes of distorted squares. Here four small distorted squares form a large distorted square, thus $m=k=4$.

3. INVARIANT CONFLATION / REGISTRATION ALGORITHM

In this section we describe an **Area Ratio Conflation Algorithm** (ARC algorithm for short). The invariance of the area relations found in the previous section is the base for this algorithm.

Two raster images are conflated by finding at least 3 matching uniquely sized regions (areas) in both images and using the center points of those regions as reference points for an affine transform calculation. There are several possible formalizations of the concept of “**matching uniquely sized regions (areas)**”.

In the ARC algorithm, we use the area ratio S_i/S_j as the matching characteristic, because of its invariance shown in the previous section. If two areas in the original image have a ratio, say 0.3, then the same ratio between them should remain the same under any affine transform. Thus, in the second image, we can compute areas of regions, their ratios S_i/S_j and search for a 0.3 ratio among them. If only one such ratio was found then centers of these regions give us two tie (control) points for building an affine transform. Finding a third region S_m in the both images with the equal ratios S_i/S_m in both images provides the third tie point needed for an affine transform. This basic idea is adjusted for the cases where more than one matching triple found. An additional uniqueness criterion is introduced in the algorithm based on the analysis of additional ratios.

Suppose there is an image that contains a large lake of some size and a small lake whose size is $1/3$ of the size of the large lake. This size ratio ($1/3$) is invariant to affine transformations. The ratio precision needs to be adjusted to the scale of least precise image. Ratios $1/3$, $1/2$ and $1/4$ could match 0.336 0.52 0.27 if images are of different scales. The algorithm uses a matching threshold for these cases. This logic of the algorithm requires: (1) an algorithm for computing area ratios and for matching ratios and (2) an algorithm for region extraction from the image. The first algorithm called the Ratio Algorithm and the second algorithm called Vectorizer are described below. The development of the second algorithm is the goal of the Step 7 of the ADTC technology.

The ratio algorithm starts from a set of regions $\{G_{1i}\}$ for image 1 and a set of regions $\{G_{2i}\}$ for image 2 extracted by the Vectorizer algorithm. The *Ratio algorithm* computes areas for each region in both images, $S_{1i}=S(G_{1i})$,

$S_{2i}=S(G_{2i})$ as a number of pixels inside of the region. Next this algorithm computes two matrixes V_1 and V_2 . Elements of matrix $V_1=\{c_{ij}\}$ are $c_{ij}=S_{1i}/S_{1j}$. Elements of matrix $V_2= \{q_{ij}\}$ are defined similarly, $q_{ij} = S_{2i}/S_{2j}$. We assume that all areas S_{1i} and S_{2i} are positive.

The area ratio algorithm consists of several steps presented below:

Step 1: Extract shapes (closed contours) in each image.

Step 2: Compute areas of each shape, order areas and select n largest shapes. For implementation we use $n=35$.

Step 3: Build a matrix as shown in Tables 1 and 2.

Table 1. Matrix of shape size ratios in Image 1

	$S_{11}=6$	$S_{12}=4$	$S_{13}=2$	$S_{14}=1$
$S_{11}=6$	1	4/6	2/6	1/6
$S_{12}=4$	6/4	1	2/4	1/4
$S_{13}=2$	6/2	4/2	1	1/2
$S_{14}=1$	6/1	4/1	2/1	1

Table 2. Matrix of shape size ratios in Image 2

	$S_{24}=7$	$S_{23}=6$	$S_{21}=4$	$S_{22}=1$
$S_{24}=7$	1	6/7	4/7	1/7
$S_{23}=6$	7/6	1	4/6	1/6
$S_{21}=4$	7/4	6/4	1	1/4
$S_{22}=1$	7/1	6/1	4/1	1

In this example matrix V_1 shown in Table 1 is computed for regions with areas $S_{11}=6, S_{12}=4, S_{13}=2, S_{14}=1$. in image 1 and matrix V_2 is computed for areas $S_{21}=4, S_{22}=1, S_{23}=6, S_{24}=7$ in image 2 (see Table 2). This matrix can also be interpreted as an oriented graph with edges marked by numbers shows in Tables 1 and 2.

Step 4: Search for common parts with at least tree rows and columns in each. We can notice that there is a common part in Tables 1 and 2 shown within the bold borders. In the case of the noise we may allow that two area ratios have, say 5% difference. This x% percentage is called a relative threshold. The complexity of the search of such common parts in two matrixes is $O(n^4)$, having n^2 elements in each matrix. Many advanced algorithms have been offered in computer vision to optimize search of common parts, e.g., see a review in Ahmadyard¹³. For our selected $n=35$, such optimization is not a high priority at this moment.

Step 5: Select a specific common part out of the set of found common parts. Some optimization algorithm can be used for such selection. Otherwise it can be a random choice.

Step 6: Identify shape match using a selected common part.

In the example the common part identifies matching shapes in two images, that is

Image 1: (S_{11}, S_{12}, S_{14})

Image 2: (S_{23}, S_{21}, S_{22})

Step 7: Compute centers of gravity (centroids) of each matched shape

Image 1: Shape centers (c_{11}, c_{12}, c_{14})

Image 2: Shape centers (c_{23}, c_{21}, c_{22})

Step 8: Compute affine transform F between shape centers found in step 7 and find vector of coefficients ($m_{11}, m_{12}, m_{13}, m_{21}, m_{22}, m_{23}$) of that transform.

Step 9: Repeat steps 5-8 for every common part found in step 4.

Step 10: Cluster vectors $\{(m_{11}, m_{12}, m_{13}, m_{21}, m_{22}, m_{23})\}$ into similarity groups, compute the number of vectors in each cluster and set up the highest priority to the largest cluster with descending priorities for other clusters. Compute centers of each cluster and find vectors that are closest to the centers.

Step 11: Apply the affine transform found in step 10 to image A and transform it to image B

Step 12: Compute shape discrepancy for each transformed shape $F(S_{11})$, $F(S_{12})$, $F(S_{13})$ and shapes (S_{23}, S_{21}, S_{22}) as the number of pixels that do not match.

Step 13: Repeat steps 11-12 for every cluster found in Step 10.

Step 14: Evaluate discrepancy. Find the best transform from Step 13.

The **conflation quality** can be evaluated by visual inspection of the conflated images and by a computational procedure based on the absolute and relative difference between matched regions found in Step 13. For instance if discrepancy is less than 10% of each shape $F(S_{1i})$ then it can be considered as an acceptable match. In general this threshold should be task-specific.

In a related work¹³ steps 5-14 are not performed, but instead a probabilistic iterative reasoning (relaxation) technique is applied, that produces matching labels to features of both images. The relaxation technique¹⁴ has been developed in a probabilistic setting¹⁵. In the first step this technique evaluates **compatibility** of the feature match based only on the information about each feature itself. On the next step this information is expanded to include information about relations between pairs of features. The next steps can use more information about relations between features if such information is available.

Different compatibility measures have been introduced: compatibility coefficients¹⁶, probabilistic relaxation that uses Bayesian Theorem to compute updates for the compatibility measure¹⁵.

The probabilistic approach is conceptually less heuristic than others, but it is difficult to obtain and operate with multidimensional probability distribution functions it requires. Thus, several heuristic assumptions in this approach have been introduced¹⁴. One of them is the assumption of independence or relations between pairs of features. In our case it is not true. For instance table 1 shows that ratios S_{11}/S_{12} , S_{12}/S_{13} and S_{11}/S_{13} , are not independent, $S_{11}/S_{13}=(S_{11}/S_{12})(S_{12}/S_{13})$.

4. SOFTWARE AND COMPUTATIONAL EXPERIMENTS

Three computational experiments with the Area Ratio Conflation algorithm described above and implemented as a Plug-in to ArcGIS are presented. The first simple example of area ratio registration/conflation is illustrated in Figure 5, where one image was modified in three ways to produce a second image. One ellipse was moved, the horizontal and vertical scales were changed by different amounts, and the image was rotated. These two images were then imported into ArcMap and registered. Figure 5 illustrates the result of the registration and shows the detection of the relocated ellipse.

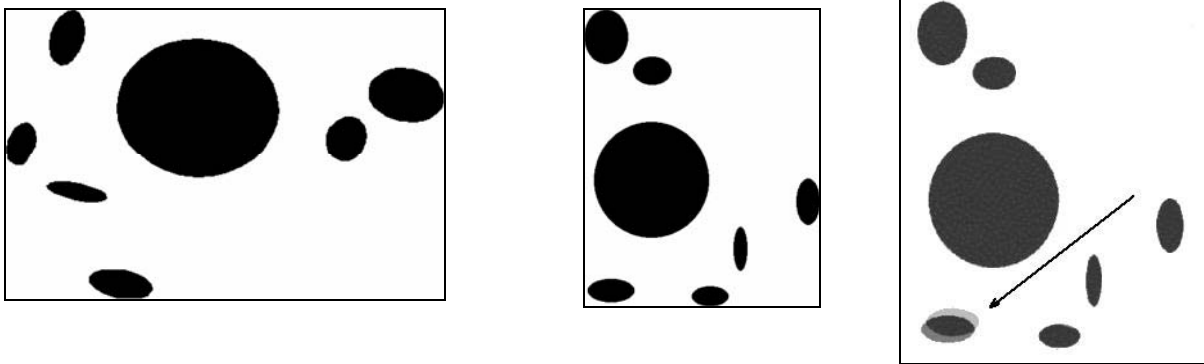
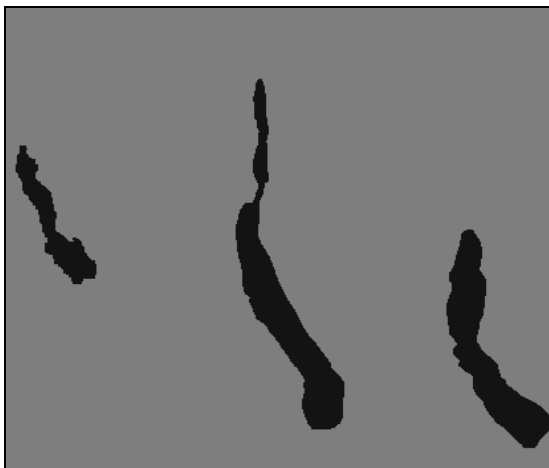


Figure 5: The registration of two slightly different images with different scale ratios and orientations. The area that was shifted is marked with an arrow.

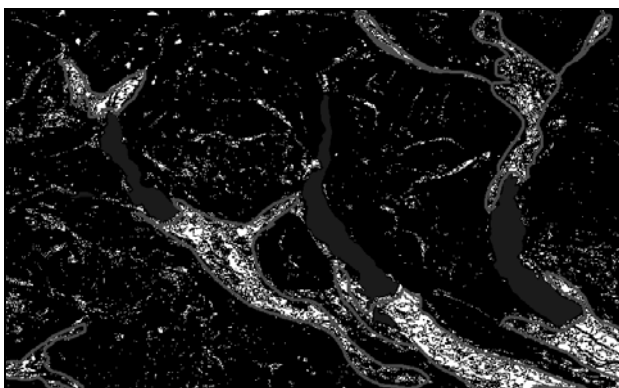
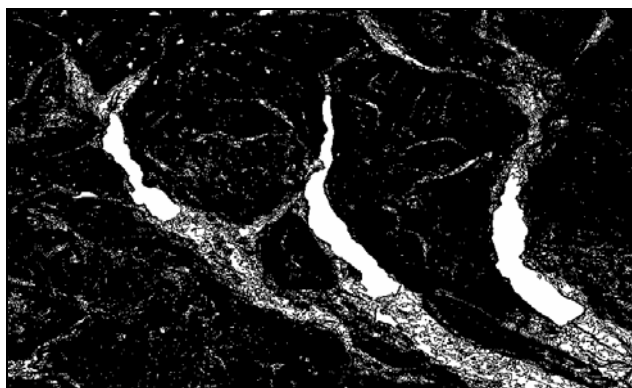
A second example shows the registration of two images of very different modalities: a digital elevation model from the Shuttle Radar Topography Mission (SRTM) and a raster Landsat satellite image. The screenshot in Figure 6 shows a

Landsat image before its co-registration with SRTM. In fact, this is a hue component of the original Landsat image shown as a grey scale image. Figure 6(b) shows the largest closed contours/areas in the same image.

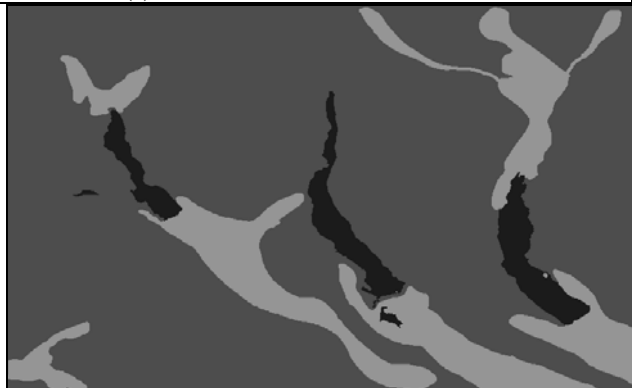


(a) Hue component of the original Landsat image shown as a grey scale image	(b) Largest closed contours/areas in the sharpened and segmented Landsat image
---	--

Figure 6. Landsat image



(a) SRTM 10m elevation contour interval	(b) SRTM relatively flat areas
---	--------------------------------



(c) SRTM sharpened flat areas	(d) SRTM flattest areas
-------------------------------	-------------------------

Figure 7. SRTM data in a visual form (10m elevation contour intervals)

Segmentation and sharpening of electro-optical (EO) images can be accomplished by a variety of methods¹³. In a simplest way it is done by setting up color thresholds for pixels. For this we use (1) hue separation, (2) statistical analysis of hue distribution, and (3) smoothing of images to decrease effect of texture and create larger areas. This is done by applying mean shift filters.

The second image, Figure 7(a), is an SRTM data set with 10 meter contours. Three reservoirs and lighter areas (where the contours are more widely spaced) are visible and marked in Figure 7(b).

The flattest areas next to the lake shore are shown in Figure 7(d). Such areas are extracted directly from SRTM by setting up elevation threshold filters. This provides sharpening and segmentation of SRTM images.

The two images are shown in Figure 8 after being imported into ArcMap. In this example, the coordinates of the upper left hand image corners were arbitrarily set to (0,0) for illustration. In practice, any image coordinate information that is available may be used and either image may be chosen as the reference for registration. The registration determined by area ratios and locations is shown in Figure 8(b). While only three areas were used in this example, similar computational experiments with ARC algorithms has shown that the method is capable of integrating images with dozens of shapes in reasonable times.

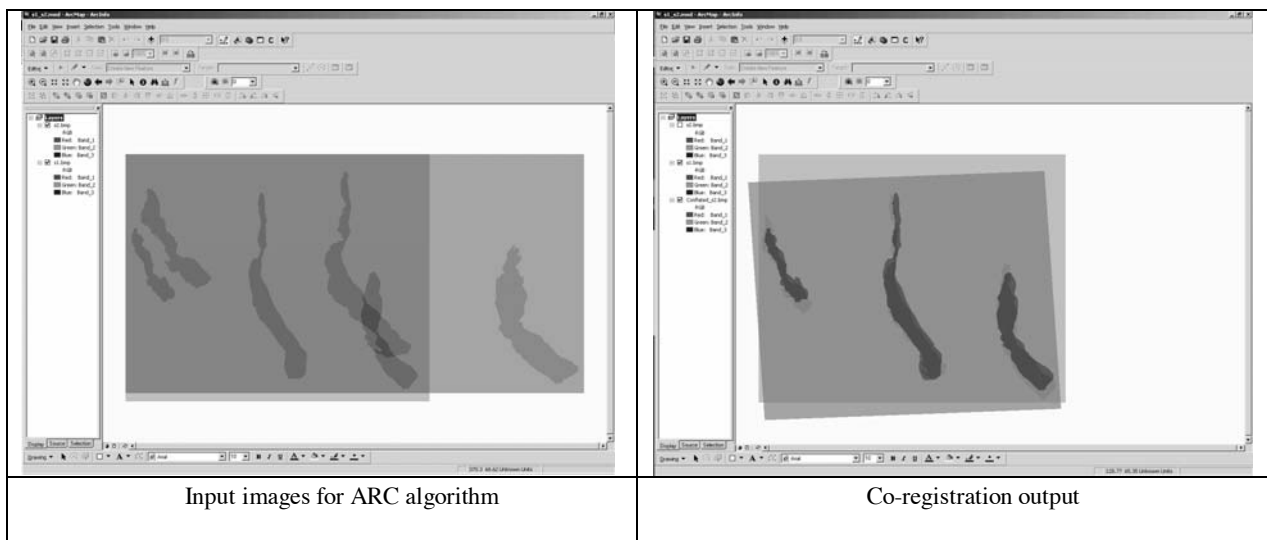
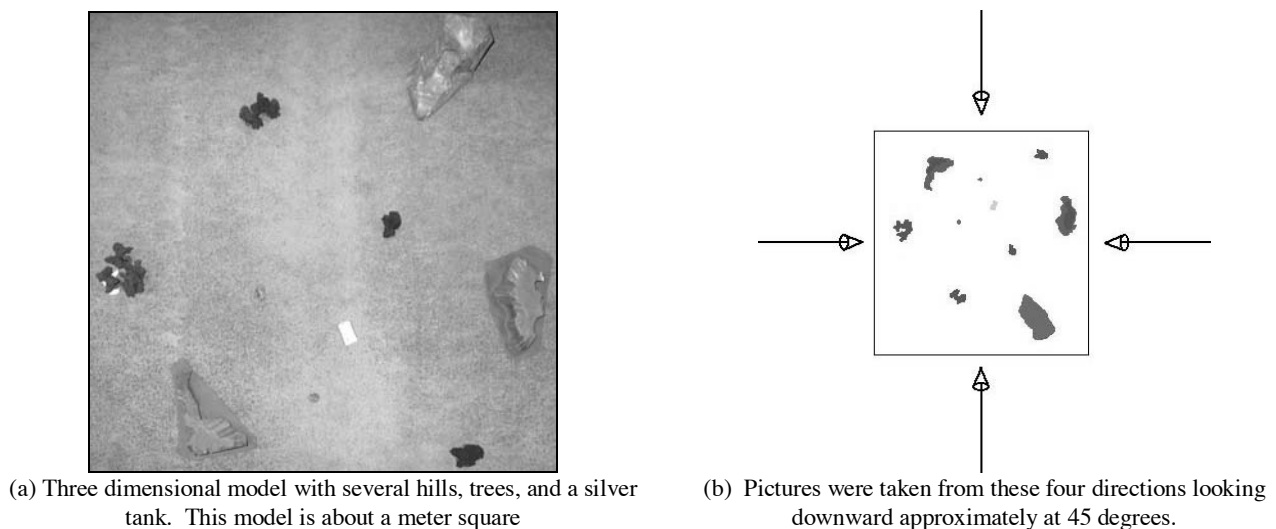


Figure 8. Images from Landsat (Figure 6b) and SRTM (Figure 6d) co-registered



(a) Three dimensional model with several hills, trees, and a silver tank. This model is about a meter square

(b) Pictures were taken from these four directions looking downward approximately at 45 degrees.

Figure 9. Experiment setting

5. CHANGE DETECTION

In the previous two examples, the registrations were calculated with affine transformations. In this example, 8 images will be considered that were taken at different camera angles before and after one element (a model tank) was moved. Affine transformations are calculated for this example, showing while they do not precisely remove the perspective differences between the images, they do provide a good solution to the problem of determining corresponding features and detecting the direction and magnitude of tank motion.

Figure 9 shows the top view of a three dimensional model of hills, trees, and a silver tank below center. Four photographs were taken looking down at about a 45 degree angle from approximately the four directions shown in Figure 10. Neither the angles nor the directions were closely control. The tank was moved and four more photographs were taken in the same way. Figure 11 shows the registration of one pair of images using the ARC ArcMap Plug-in. Eight photographs are shown on top of one another in Figure 12. While the areas are not exactly aligned, they are close and the movement of the silver tank is evident.

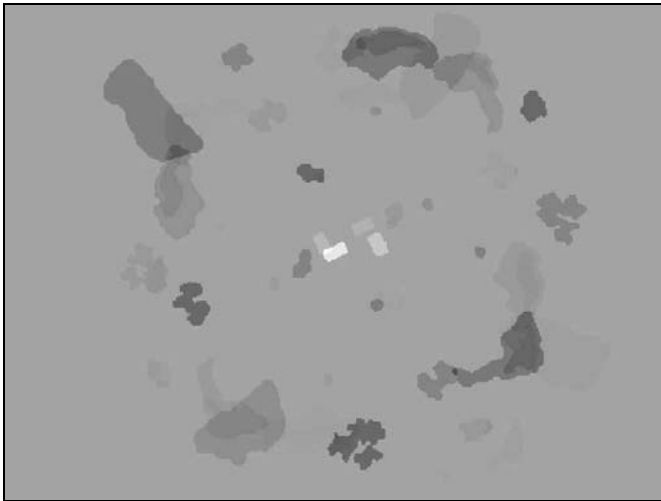


Figure 10. Four sharpened photographs of the scene shown above in Figure 8. These superimposed images have the original camera orientations.

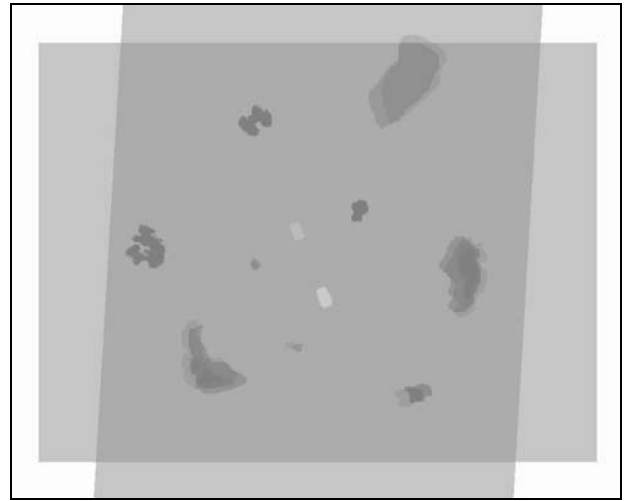


Figure 11. The registration of one pair of before and after images.

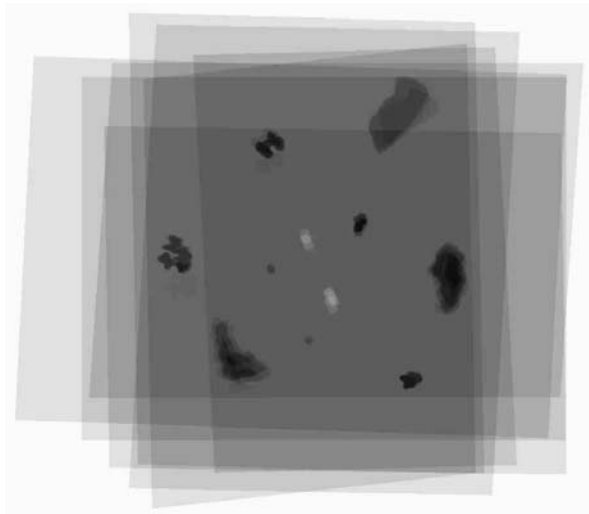


Figure 12. Registration of 7 images to one selected as a "standard".

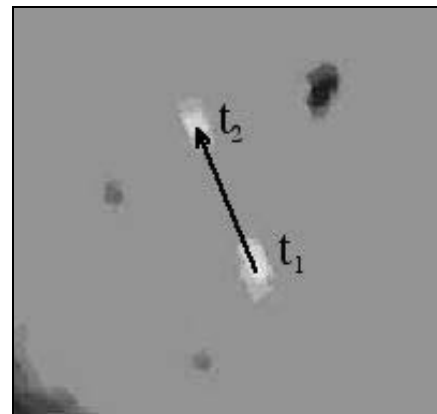


Figure 13. Close up of figure 12 showing the quality of the registration and arrow indicating movement.

Selecting one image as reference and registering the remaining 7 to it gives the result shown in Figure 12. Figure 13 is a close up of the tank area showing the quality of the registration and an arrow estimating the direction and distance of movement.

6. GENERALIZATIONS

The structure of an SRTM digital elevation model in Figure 14 illustrates how features can be constructed using both contours and gradients of contours, following selected drainages and filling a closed contour to create a distinctive area. Not only are the individual structures of these features unique, their spatial relationships also define an algebraic structure. These combinations are natural generalizations of the three examples presented earlier and illustrate just one generalization of our algebraic technique.

The ARC algorithm is a part of general Algebraic Framework^{17,4}. The matrix representation used in this algorithm is important because it permits us to convert the situation to a generic algebraic system framework, with algebraic systems $A_k = \langle A_k, R_k, \Omega_k \rangle$, where signature Ω_k contains the operator $V_k(a_i, a_j)$ represented as a matrix V_k and handles the conflation problem uniformly. Operators with more arguments are also possible. From this point uniformity permits us to use a single and already implemented algorithm to search for matching features in the images. It does not matter for the algorithms in algebraic form whether elements of A_k are straight-line segments, polylines, areas, other features, or complex combinations of any of them. Elements of A_k also can be numeric characteristics of image components such as a size of region i in image k , S_{ki} and their ratios used in ARC. This approach generalizes graph based relaxation techniques^{13, 14, 15, 16}.

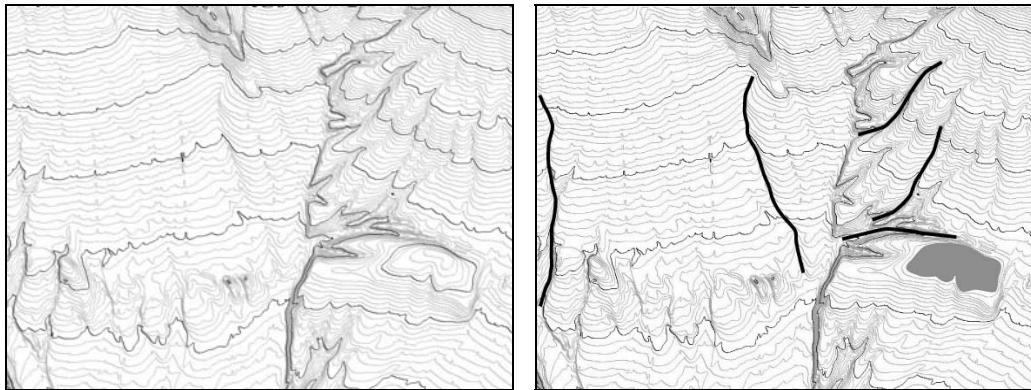


Figure 14: Contours of a SRTM digital elevation model with polyline and area features.

7. AFFINE INVARIANCE OF DISTANCE RATIOS IN CENTROID LINES

The method can be generalized by adding other affine invariants, such as distance ratios^{13,18}. Below we discuss one version of such ratios. In Figure 15 image (b) is a result of an affine transform of image (a). Lines connect centroids of areas. We consider intervals AB and JL on the line that connect two centroids in image (a). Similarly there are intervals $A'B'$ and $J'L'$ on the corresponding line in image (b). We compute lengths of these intervals, $|AB|$, $|JL|$, $|A'B'|$, and $|J'L'|$.

Definition. Ratios $|AB|/|JL|$ and $|A'B'|/|J'L'|$ are called distance ratios in centroid lines.

Statement. If Image (b) is a result of an affine transform of the image (a) then relation (2) takes place

$$|AB|/|JL| = |A'B'|/|J'L'| \tag{2}$$

We will call relation (2) a direction invariance relation, because ratios $|AB|/|JL|$ and $|A'B'|/|J'L'|$ indicate relative width of shapes in a specific direction. In this case this is the direction to the center of another shape.

Proof. An affine transform preserves parallel lines and segments of a single line are transformed to segments of the single line too. Assume that an origin of the coordinate system is located in point A and x coordinate follows line AB. Then the length of AB is the x coordinate of point B, $|AB|=x_B$. The length of JL is x_L-x_J , $|JL|=|x_L-x_J|$

$$|AB|/|JL|=|x_B|/|(x_L-x_J)| \tag{3}$$

The coordinates of points, A,B,J and L are as follows $A=(0,0)$, $B=(x_B, 0)$, $J=(x_J,0)$, $L=(x_L,0)$. Assume an affine transform: $x'=m_{11}x+m_{12}y+m_{13}$ and $y'=m_{21}x+m_{22}y+m_{23}$ then $A'=(m_{13}, m_{23})$, $B'=(m_{11}x_B+m_{13}, m_{12}x_B+m_{23})$, $J'=(m_{11}x_J+m_{13}, m_{12}x_J+m_{23})$, $L'=(m_{11}x_L+m_{13}, m_{12}x_L+m_{23})$ and $|A'B'|=|m_{11}x_B, m_{12}x_B|=|x_B| \cdot \|m_{11}, m_{12}\|$, $|J'L'|=|m_{11}(x_L-x_J), m_{12}(x_L-x_J)|=|(x_L-x_J)| \cdot \|m_{11}, m_{12}\|$

$$|A'B'|/|J'L'|=|x_B|/|(x_L-x_J)| \tag{4}$$

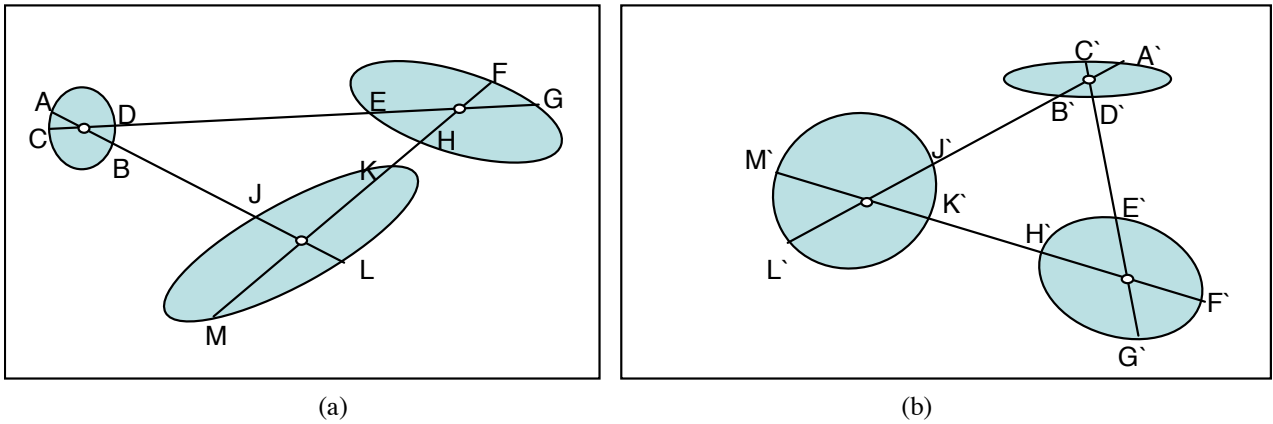


Figure 15. Affine transformed images with distance ratios on center lines.

Combining formulas (3) and (4) we obtain the statement. This lemma gives us an important affine invariant parameter for the algorithm. We will call these distances diameters and their ratios diameter ratios.

The ARC algorithm presented above can be generalized using distance ratio in centroids. We do not use a heuristic compatibility measure offered in Ahmadyard¹³ to incorporate this ratio. We use this ratio to resolve ambiguity in area match provided by area ratios in ARC algorithm to speed up search for match. We also use distance ratio to increase a confidence in match provided by area ratios. The explanation for this sequential approach is that area ratios are generally more robust and should have precedence.

8. SUMMARY

Imagery integration has a variety of open questions in image registration, conflation, and search. A new promising approach is based on the algebraic paradigm that differs from the more traditional geometric and topological approaches. In this paper we presented a new algebraic method based on ratios of areas of closed contours. This method is invariant to disproportional scaling and any general affine transform. Even when images are not related by an affine transformation, this technique may often be usefully applied. It is applicable to images that contain three or more matching shapes. The algorithm automatically discovers matching shapes. Computational experiments had shown that the method is capable of integrating images with dozens of shapes in reasonable times. The algorithm has been developed using two methodologies: Algorithm Development Technology for Conflation and Algebraic Relational Invariant paradigm. The algorithm has been implemented as an ArcMap Plug-in to make it more widely useful, but there is nothing in the ARC or algebraic method that uses or depends on the proprietary features of ArcMap.

ACKNOWLEDGEMENTS

The authors gratefully acknowledge that this research has been supported by National Geospatial-Intelligence Agency through its Academic Research Program Grants NMA401-02-1-2006 and NMA401-02-1-2007.

REFERENCES

1. Zitová B., Flusser J., Image registration methods: a survey, *Image and Vision Computing*. 21 (11), 2003, pp. 977-1000.
2. Kovalerchuk, B., Sumner W., Curtiss, M., Kovalerchuk, M., and Chase, R., Matching Image Feature Structures Using Shoulder Analysis Method, In: Algorithms and technologies for multispectral, hyperspectral and ultraspectral imagery IX. Vol. 5425, International SPIE military and aerospace symposium, AEROSENSE, Orlando, FL, April 12-15, 2004.
3. Kovalerchuk B., Schwing J. (eds.), *Visual and Spatial Analysis: Advances in Data Mining, Reasoning and Problem Solving* (Eds.), Springer, 2005.
4. Cobb, M. Chung, M.,Foley, Petry. F., Shaw, K., and Miller, H., A rule-based approach for the conflation of attributed vector data, *GeoInformatica*, 2/1, 1998, 7-36.
5. Jensen J., Saalfeld, A., Broome, F., Price, K., Ramsey, D., and Lapine, L. Spatial Data Acquisition and Integration, 2000, NSF Workshop GIS and Geospatial Activities. http://www.ucgis.org/research_white/data.html
6. Doytsher, Y. Filin, S., Ezra, E. Transformation of Datasets in a Linear-based Map Conflation Framework, *Surveying and Land Information Systems*, Vol. 61, No. 3, 2001, pp.159-169.
7. Edwards D., Simpson J. Integration and access of multi-source vector data, In: *Geospatial Theory, Processing and Applications*, ISPRS Commission IV, Symp.2002, Ottawa, Canada, July 9-12, 2002, 8.Ref.3, Ch.17-19.
9. Brown, L. A Survey of Image Registration Techniques, *ACM Computing Surveys*,vol.24 (4),pp. 325--376,
10. Shah, M., Kumar, R., (Eds.) *Video Registration*, Kluwer, 2003.
11. Terzopoulos D., Studholme, C., Staib, L., Goshtasby A., (Eds) *Nonrigid Image Registration*, Special issue of *Computer Vision and Image Understanding Journal*, vol. 89, Issues 2-3, pp. 109-319, 2003
12. Wang, J., Chun, J., and Park, Y.W. GIS-assisted image registration for an onboard IRST of a land vehicle. *Proc. SPIE* Vol. 4370, p. 42-49, 2001.
13. Ahmadyfard, Object recognition by region matching using relaxation with relational constraints, Ph.D Dissertation, Univ. of Surrey, UK, 2003. ftp://ftp.ee.surrey.ac.uk/pub/vision/papers/Ahmadyfard_thesis.pdf
14. Rosenfeld,A., Hummel, R. Zucker, S., Scene labeling by relaxation operations, *IEEE Trans. on System and Cybernetics*, pp. 420-433, 1976
15. Christmas, W., Kittler, J., Petrou, M., Structural matching in computer vision using probabilistic relaxation, *IEEE Trans. on pattern analysis and machine intelligence*, pp. 749-764, 1995.
16. Hummel, R., Zucker, S. On the foundation of relaxation labeling process. *IEEE Trans. Pattern Analysis and Machine Intelligence*, 5(3):267-286, May 1983.
17. Mal'cev A.I. *Algebraic Systems*, Springer-Verlag, New York, 1973
18. Matsakis, P. Keller, J., Sjahputera, O., Marjamaa, J., The Use of Force Histograms for Affine-Invariant Relative Position Description, *IEEE Transactions on Pattern Analysis And Machine Intelligence*, Vol. 26, No. 1, January 2004.